Hindawi
Journal of Sensors
Volume 2017, Article ID 8365189, 10 pages
https://doi.org/10.1155/2017/8365189

Research Article

Detection of *Aeromonas hydrophila* Using Fiber Optic Microchannel Sensor

Samla Gauri,[1] Zurina Zainal Abidin,[1] Mohd Firdaus Kamuri,[1] Mohd Adzir Mahdi,[2] and Nurul Amziah Md Yunus[3]

[1]*Department of Chemical and Environmental Engineering, Faculty of Engineering, University Putra Malaysia, Selangor, Malaysia*
[2]*Department of Computer and Communication Systems Engineering, Faculty of Engineering, University Putra Malaysia, Selangor, Malaysia*
[3]*Department of Electrical and Electronic Engineering, Faculty of Engineering, University Putra Malaysia, Selangor, Malaysia*

Correspondence should be addressed to Zurina Zainal Abidin; zurina@upm.edu.my

Received 10 August 2016; Revised 11 November 2016; Accepted 4 December 2016; Published 4 January 2017

Academic Editor: Stephane Evoy

This research focuses on the detection of *Aeromonas hydrophila* using fiber optic microchannel biosensor. Microchannel was fabricated by photolithography method. The fiber optic was chosen as signal transmitting medium and light absorption characteristic of different microorganisms was investigated for possible detection. Experimental results showed that *Aeromonas hydrophila* can be detected at the region of UV-Vis spectra between 352 nm and 354 nm which was comparable to measurement provided by UV spectrophotometer and also theoretical calculation by Beer-Lambert Absorption Law. The entire detection can be done in less than 10 minutes using a total volume of 3 μL only. This result promises good potential of this fiber optic microchannel sensor as a reliable, portable, and disposable sensor.

1. Introduction

Aeromonas hydrophila is a known free living pathogen that not only causes infections to human and animal but also influences the economics of fisheries department. It is a Gram-negative aerobic and facultative anaerobic, oxidase-positive motile bacterium mostly found in aquatic environments especially fresh stream and ponds. This bacterium contributes to internal infectious conditions like dermal ulceration, rotting of tails, inflammation, exophthalmia, scale protrusion, and others in fish species [1] especially *Cyprinus carpio* and *Carassius auratus*. This has caused high mortality and economic losses of fish farming [2]. These bacteria can cause pathogenesis to human too through freshwater fish hemorrhagic, zoonotic diseases and also food-borne infections. The microorganism may require highly appropriate antimicrobial treatment to control potential serious consequences [3] due to its resistance towards the normal antimicrobials (*ampicillin, cephalosporin,* and *cloxacillin*).

Pathogen early detecting tool would be extremely useful to recognize *A. hydrophila* at an early stage to prevent diseases and infections to animals and human and also minimize the economic impact it brings to fish farming industry. Detection of pathogen demands a highly efficient, sensitive, and rapid tool due to its pathogenicity and fast infection rate. In the past years, several methods have been developed for detection of *A. hydrophila* such as identification based on molecular detection (e.g., polymerase chain reaction [PCR] method) and culture based detection method, which can be laborious and time-consuming [4–6]. Numerous probes like DNA microarray [7], immunological tool (based on monoclonal antibody [Mab]) [8], and electronic nose (based on changes of volatile patterns produced by *A. hydrophila*) [9] were also constructed in recent years. Even though these unique systems were relatively sensitive and accurate, a need for a direct and rapid detection tool with lower detection limit is still essential to compete with increasing rate of infections.

The advancement in molecular biology, microelectronics, and optical and computer technologies has led to the development of miniaturized biorecognition system that can deliver a rapid result with simple methods and observations [10]. This miniaturized device can be used as an in-line direct

detection and also has in vivo measurement applications [11]. Emerging method using optical fiber arrays with multiwavelength ultraviolet to visible (UV-vis) spectra provides a powerful and low cost substrate for creating high-density sensing systems to address a variety of biological problems [12–15]. An optical fiber in sensor technology, especially in detection of microparticles, delivers a very high sensitivity either with applications of light-emitting diodes (LED) or with laser diode (LD) as the excitation [16].

Microfluidic system is a system that processes or manipulates small (10^{-9} to 10^{-18} litres) amounts of fluids, using channels dimensions of tens to hundreds of micrometres [17]. The microfluidic system offers so many advantages: the ability to use very small quantities of samples and reagents and high resolution and sensitivity; low cost; less times for analysis; and small footprints for the analytical device [18]. For certain applications, only small amounts of sample analyte might be usable. The analyte has to be exploited as much as possible. Several attempts have been made to fabricate focusing system on different materials. Numerous microlens materials and corresponding technologies have been demonstrated, like polymer [19–22], silica [23, 24], diamond [25], and sol-gel [26, 27]. The main challenges faced by many experiments are the fabrication involving high-priced charges and complex processes and equipment [28].

Fiber optic biosensor can be an efficient method for reliable detection of pathogen in the effort to reduce its fatal effect. Several studies have successfully employed biosensors to detect *E. coli* [29–32] including the development of fluorescent based fiber optic biosensor hybridized with DNA sequences to detect oligonucleotides as an indication of *E. coli* infection. For instance, Leung et al. [33] demonstrated the detection of *Helicobacter pylori* at near-infrared region (785 nm) via oligonucleotide cross-linked to a fluorescent fiber optic sensor. The detection was near infrared region (785 nm) with oligonucleotide cross-linked to the sensor. In this research, a direct analytical tool for detection and identification of *A. hydrophila* using UV-Vis spectra based fiber optic biosensor is proposed. Optimization work on this detecting tool is performed in order to produce a sensitive and rapid detection without the need of focusing system. The detection of microorganism is determined based on their absorbance spectrum and region.

2. Materials and Methods

2.1. Preparation of Microorganism. *A. hydrophila* was used to test the suitability and efficiency of the fiber optic biosensor. Strains of *A. hydrophila* were obtained from Science and Technology Research Institute for Defence, Malaysia Ministry of Defence, and Department of Fisheries, Ministry of Agriculture and Agro-Based Industry, Malaysia (Penang Branch). The strain was grown on Tryptic Soy Agar (TSA, Oxide) and incubated overnight. The sample was harvested and washed using sterilized deionized water and the growth curves were measured at 610 nm by using UV spectrophotometer. The measured growth curves of these microorganisms at particular wavelengths (Table 1) were used to select their physiological stages for subsequent optical measurement.

Table 1: Selected sample phases based on growth curve obtained by spectrophotometer for absorbance measurements.

Samples	Phases	Optical Density (OD) at 610 nm	Hour
A. hydrophila	Lag	0.40	3
	Exponential	0.65	6
	Stationary	0.94	9

2.2. Design and Fabrication of the Fiber Optic Microchannel. The microchannel was designed and fabricated by photolithography method as shown in Figure 1. First, the mask for the chamber was designed using AutoCAD 2011 (Figure 2) and printed on a high resolution transparency sheet. The width of the fiber grooves was to fit to the diameter of the fiber (125 μm). The sizes of microchannel and reservoir diameter are of 0.1 cm × 5 cm and 0.18 cm, respectively. The detecting reservoir was designed to collect 3 μL of sample volume. Next, the glass substrate was cleaned using methanol, propanol, and isopropyl to remove impurities, contamination, and particulate matter on the surface. After rinsing, the substrate was immediately placed in the oven at 200°C and held there for a fortnight. A small amount of photoresist Ordyl Alpha 940 was placed onto the substrate. The designed mask was aligned accurately on the photoresist coated substrate and exposed under high intensity of UV light for about 20 seconds. The substrate was soft baked for about half an hour at 100°C on a hotplate.

After that, the underlying material was removed. The substrate was immersed in a developer solution for a few seconds and then washed with deionized water. Then, the substrate with the designed pattern was hard baked for one hour at 100°C to solidify and harden the resist on the surface. Next, by using a microscope, fiber optic was placed and aligned into the fiber grooves made on the substrate. The fiber optic was glued permanently into the grooves with fast cure epoxy in order to avoid any mechanical movement that leads to the issue of misalignment. Fiber optic was used as a medium to transmit and receive the light signal for detection and identification of the particular microorganisms. Fiber optic has an excellent capability in delivering and receiving light signals, as the attenuation loss was less during signals transmission. Next, the inlet and outlet tubing were fixed onto the substrate. Finally, the microchannel was enclosed with a transparent lid/glass cover slide.

2.3. Absorbance Measurement by Fabricated Fiber Optic Microchannel. As illustrated in Figure 3, the microchannel was connected to spectroscopy system by bare fiber adapter. The spectroscopy system comprised light source with wider spectral region of wavelength (200 to 900 nm) and integrated JAZ photodetector (*JAZ*, Ocean Optic, USA) in a single unit which count the photons from the light transmitted from the fiber optic. The light source from spectroscopy with the potential of 5 V was transmitted to microchannel through

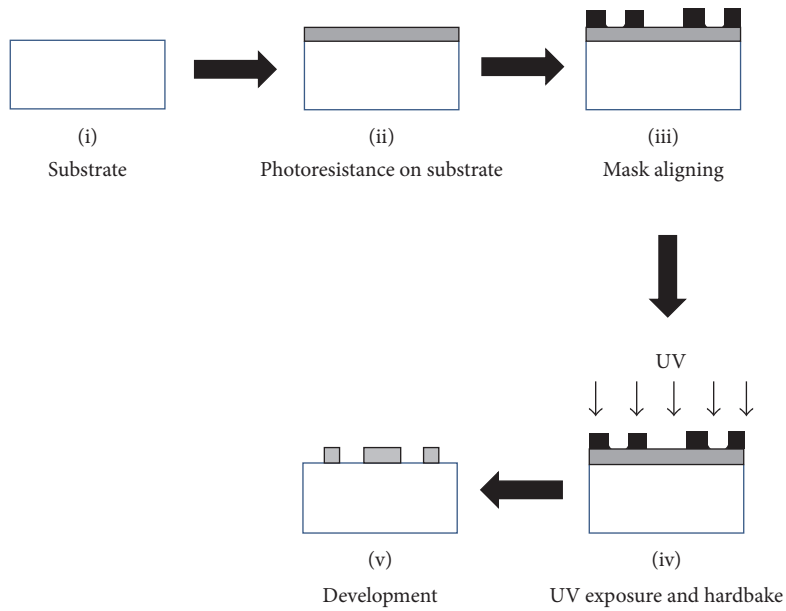

Figure 1: Photolithography method fiber optic microchannel fabrication.

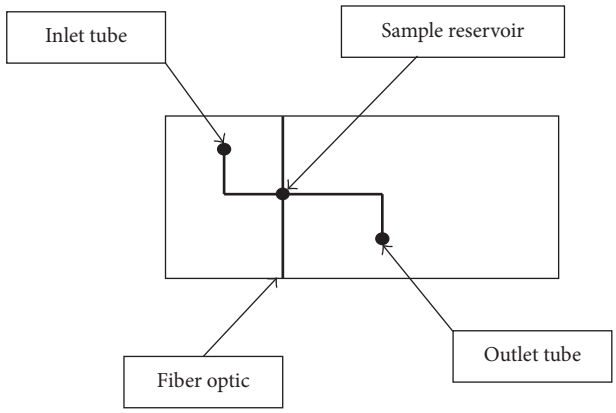

Figure 2: The designed mask printed on high resolution transparency sheet.

fiber optic. It takes 10 minutes to stabilize the spectrum before the absorbance rate was acquired and collected by fiber optic. Absorbance unit of distilled water was used as the reference point for the microchannel reading. The sample was then injected to the microchannel through inlet tubing using syringe pump. The absorbance spectra (AU) of sample as function of time for continuous wavelength from 200 nm to 900 nm were recorded for different physiological stages from lag phase of 3×10^7 cells mL^{-1}, exponential phase of 5×10^7 cells mL^{-1}, and stationary phase of 7×10^7 cells mL^{-1}. When microbes passed across the light signal, the desired microbe will be illuminated and excited at different wavelength compared to other microbes. The most absorbed region was chosen as an optical detection region of particular microorganism. Continuous spectra of the sample absorbance will be collected and analyzed.

2.4. Validation Measurement. UV spectrophotometer (Genesys 10 UV, Thermo Electron Corporation) was used to validate the max/peak absorbance region obtained from fiber optic microchannel in order to compare and justify the experimental results. The UV spectrophotometer measurement of the samples was performed by taking the values of absorbance unit at different interval of growth time. The wavelength selected as the set point for UV spectrophotometer was based on highest absorbance region (wavelength) of the sample during microchannel measurements. The selected wavelengths based on microchannel measurement for *A. hydrophila* included 352 nm 353 nm and 354 nm. The collected data through UV spectrophotometer and experimental works were analyzed based on two statistical measurements. Firstly, the coefficient of determination (R^2) which indicates how well the data fit or regression line approximates the real data points. Then standard deviation was calculated to evaluate the accuracy of the data to expected value.

Further validation to the UV spectrophotometer measurement was done by calculating the concentration for absorption unit of the corresponding samples using the Beer-Lambert absorption law [37] as follows:

$$A(\lambda) = \varepsilon(\lambda)\, bc, \tag{1}$$

where A is absorbance, ε is molar absorptivity, b is path length of sample, and c is concentration of sample. Equation (1) states the relationship between absorption and the concentration of the microorganisms. The absorptivity coefficient, ε, is a constant used to measure amount of particles which absorb light at a particular wavelength [38]. It is important to note that the linearity of Beer-Lambert Law is limited by chemical and instrumental factors such as deviations in absorptivity coefficients at high concentrations, scattering of light due to particulates in the sample, fluorescence sample, changes in refractive index at high analyte concentration, shifts in

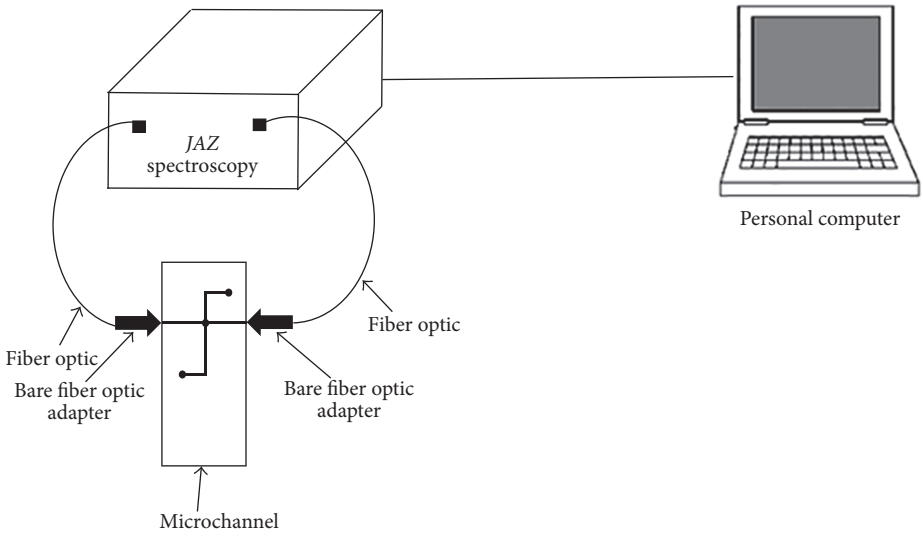

Figure 3: Experimental setup for fiber optic microchannel with *JAZ* spectroscopy.

chemical equilibria as a function of concentration, stray light, and nonmonochromatic radiation.

3. Results and Discussion

3.1. Transmission Measurement by Fiber Optic Microchannel. Transmittance is the amount of light transmitted expressed as a fraction of the amount of light striking an object. Transmittance of light at specific wavelength through the fiber optic can be explained by Beer-Lambert Law of transmittance which described the intensity ratio of the radiation coming out of the sample to the intensity of incident radiation. The results obtained from transmission measurement were used to explain the efficiency of microchannel to conduct the overall experiments. After about 10 minutes of signal stabilization, the maximum transmittance rate of the microchannel was measured at approximately 85%–92% intensity (Figure 4). Hence, the efficiency of the microchannel to read absorbance was 0.85 with 0.15 of uncertainty. This finding, while preliminary, showed that there was enough light introduced from the light source into the optical fiber and collected by the detecting device. There are possible alternatives to improve efficiency of the microchannel among others which are application of high output power light sources and the use of higher numerical aperture and higher core diameter of optical fibers. These solutions may lead to obtaining much higher light-coupling coefficient from light source into optical fiber and from optical fiber to detector. However, the work and results are limited due to the unavailability of equipment.

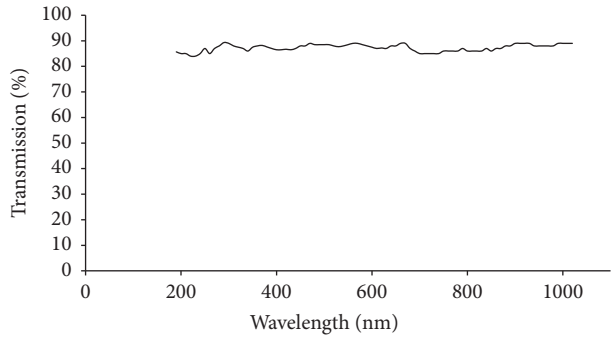

Figure 4: Transmittance measurement by fiber optic microchannel for continuous wavelength.

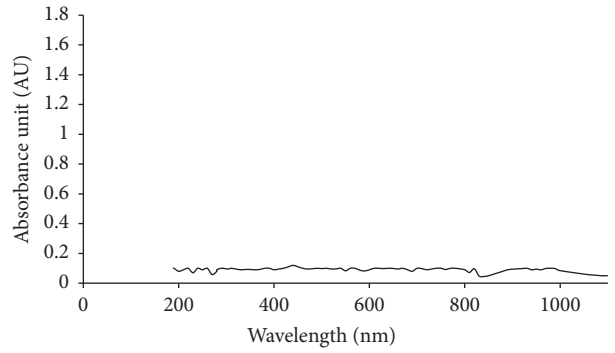

Figure 5: Absorbance spectra of reference point (distilled water) read by fiber optic microchannel.

3.2. Absorbance Spectra of A. hydrophila for Various Physiological Phases. In order to set the reference point for the absorbance spectra, distilled water was introduced into microchannel by using syringe pump. The system was then allowed to stabilize for 10 minutes to acquire the absorbance unit. The absorbance unit (AU) of UV-Vis spectrum of clear and contaminant-free (particular matter-free) distilled water was 0.1 (Figure 5). Distilled water scatter but does not absorb ultraviolet and visible region but absorbs IR radiation fairly well [39, 40]. Then, *Aeromonas hydrophila* sample was injected to the microchannel and the continuous absorbance spectra of samples were measured as function of wavelength for different physiological stages of microorganism.

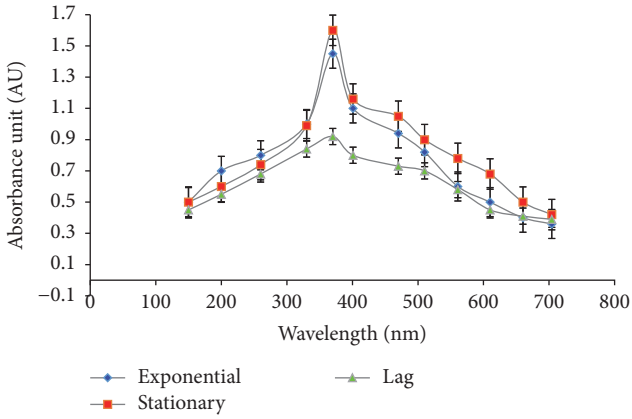

Figure 6: Absorbance spectra with error bar for *A. hydrophila* for their physiological stages by fiber optic microchannel.

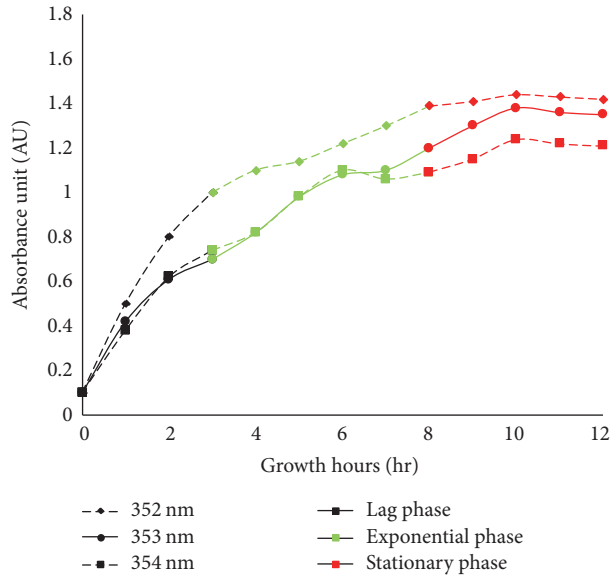

Figure 7: Absorbance values of *A. hydrophila* for different phases at particular growth interval measured by UV spectrophotometer based on selected wavelength of 352 nm, 353 nm, and 354 nm (determined earlier through microchannel measurement).

The absorbance as a function of wavelength was shown in Figure 6 which falls within the region of ultraviolet and visible range. This is good since this will help to reduce interference of absorbance from distilled water. The peak absorbance spectra for all the three physiological phases remained within region of 352 nm to 354 nm. Lag phase of *A. hydrophila* recorded the peak absorbance of 1.15 at the region of 354 nm and exponential phase gave 1.54 peak absorbance at the region of 352 nm. Subsequently, *A. hydrophila* at stationary phase absorbed most with 1.64 absorbance at the 353 nm region. The absorbance unit was increasing as the physiological phases of sample change. In short, the entire *A. hydrophila* can be detected at 352 nm to 354 nm although there would be difference in absorbance by using the designed fiber optic microchannel.

From the observation, sample absorbed most at stationary phase followed by exponential phase and then lag phase at approximately similar region of wavelength. Different optical properties of each microorganism can be used to identify the sample at different stages, shapes, sizes, and chemical compositions [41]. In the lag phase, cells adapt to growth conditions and undergo changes in their chemical composition. The exponential phase is a period characterized by cell doubling where cells increase exponentially. As the stationary phase results from a situation in which growth rate and death rate are equal due to depletion of essential nutrients, thus the growth eventually stops before it decreases. Thus, measureable properties of cells such as cell population, DNA, chemical properties, energy, and photopigments will be changing according to cell growth rate. These differences were able to be detected with optical measurement and differentiated by absorbance unit for each phase. When the cell population increased, the absorbance unit also increased as in stationary and exponential phases but still can be found in approximately similar region. A slight difference in detection region of wavelength for each phase might be due to changes of cell population and energy level of absorption. Furthermore, microchannel results can be affected by external noise or microbending of fiber optic during experiment setup.

3.3. Validation of Experimental Findings. In this section, the validation of the microchannel experimental results was done by comparing with UV spectrophotometer reading and also with theoretical calculation using Beer-Lambert Law of Absorption.

First validation was done with respect to UV spectrophotometer reading. The absorbance values of the microbial growth after 12 hours were measured at the selected wavelengths (chosen based on the max/peak absorbance region recorded by the microchannel system earlier). The measured graph using spectrophotometer was summarized in Figures 7 and 8. Based on the experimental observation there was significant positive correlation between UV spectrophotometer readings and experimental findings using fiber optic microchannel. The validation measurement for detection region of *A. hydrophila* was promising as UV spectrophotometer is able to produce favorable growth curve shape with maximum absorbance unit when compared with a typical growth curve shape.

A crude simulated growth curve (Figure 8) was generated based on best-fit curved trend-line method together with the measurement of coefficient of determination (R^2) to indicate how well the data approximate the real UV spectrophotometer data points. Results showed that data taken at wavelength of 352 nm displayed most acceptable reading of 1.54 AU and the determination of coefficient (R^2) of 0.9688. Hence it is concluded that the higher R^2 value at 352 nm means the UV spectrophotometer data fitted better to data collected by microchannel compared to other wavelengths. Further analysis of standard deviation revealed the accuracy of the data to expected value as shown in Table 2. A low standard deviation was found upon calculation at wavelength of 352 nm compared to the other wavelength region. Hence,

Table 2: Comparison of absorbance units for microchannel and UV spectrophotometer of *A. hydrophila* with standard deviation of each set of data values.

Phases	Wavelength (nm)	Absorbance unit (AU) for UV spectrophotometer	Absorbance unit (AU) for microchannel	Standard deviation (±)
Lag	352	1.00	0.95	0.025
	353	0.80	1.00	0.100
	354	0.85	1.15	0.150
Exponential	352	1.50	1.54	0.020
	353	1.40	1.35	0.025
	354	1.30	1.25	0.025
Stationary	352	1.57	1.53	0.020
	353	1.50	1.64	0.070
	354	1.40	1.58	0.090

Table 3: Coefficient of determination, R^2 obtained for various samples by previous studies.

Sensor technology	Analyte	Coefficient of determination, R^2	Reference
CCD camera	Ovarian cancer HE4 biomarker	0.93	[34]
Fiber optic	Aromatic hydrocarbon	0.993	[35]
Visual/no sensor	Food pathogens	0.98	[36]

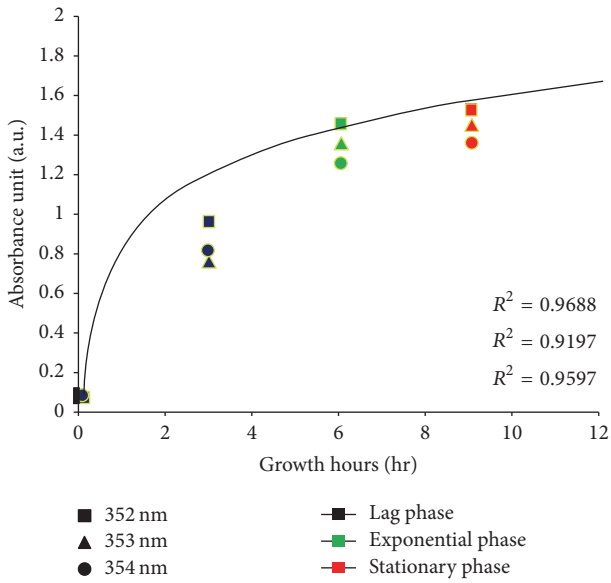

Figure 8: Simulation of *A. hydrophila* growth curve microchannel data based on best-fit trend-line method. Evaluated coefficient of determination (R^2) on how well the fitted curve approximates the real data points of microchannel and other regions obtained from UV spectrophotometer.

based on R^2 and standard deviation values, the absorbance readings are shown to be closer to microchannel data at wavelength 352 nm and hence it can be deduced that *A. hydrophila* can be detected most reliably at the region of 352 nm. A summary of the various sensor technologies that achieved high accuracy is shown in Table 3. However, none of these works tested on *Aeromonas hydrophila*. The closest work to ours was done by Richards and Watson [42] whereby they detected *A. hydrophila* at the wavelength of 364 nm which is slightly different to our findings in this work.

Next the experimental results were compared with theoretical value calculated using Beer-Lambert Absorption Law. The absorptivity coefficient, ε, is a constant that is essential to the solute itself and is measure of a degree to which particles in the solute absorb light at a particular wavelength. Initially, the absorption coefficients (ε) at different wavelengths were calculated. The choice of wavelength depends fundamentally on the values at which the spectra show the greatest difference and can be easily selected from the maxima on this curve. This calculation was performed by constructing calibration curves (Figure 9(a)) at different concentration levels (0–6 × 10^7 cells/mL). The absorption coefficients were calculated from the slope of concentration of each fraction against the absorbance measured at different wavelengths. The value obtained for the absorption coefficients was 1.25 × 10^{-8} mL cm^{-1} $cell^{-1}$. With the known absorption coefficients for the different wavelengths, the absorbance can be measured for each concentration. Figure 9(b) shows the absorption measured from fiber optic experimentally and also calculated by Beer-Lambert Law for exponential phase as a mean for comparison. By calculation, the peak absorbance was found to be 400 nm with 1.2 absorbance value while fiber optic microchannel gave absorbance of 1.54 at 352 nm.

These deviations from the Beer-Lambert Law can be classified into real deviations, chemical deviation, and instruments deviation. Since the analyte used was microorganism, thus the deviations are mostly from instruments and real deviations. Beer-Lambert Law is capable of describing absorption behavior of solutions containing relatively low amounts of solutes dissolved in it. At high analyte concentrations, it interacts with solvents and the analyte begins to behave differently due to interactions with the solvent

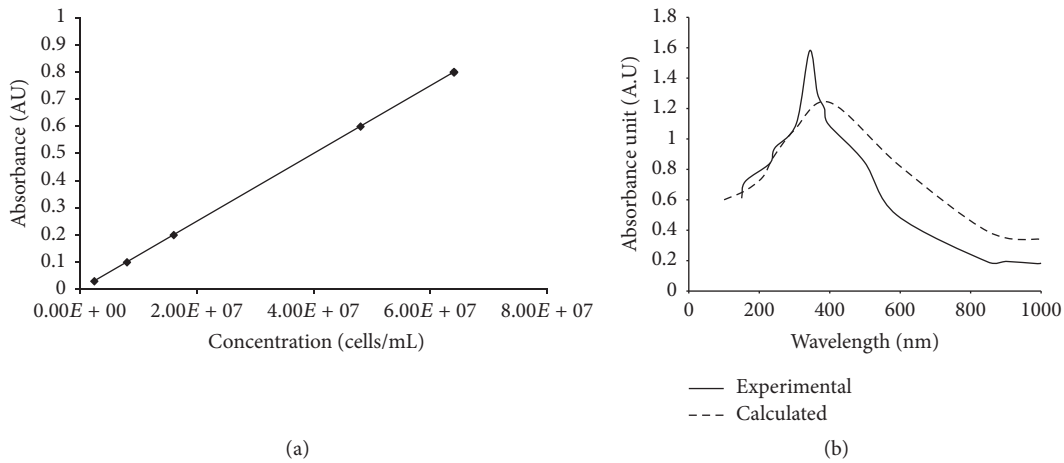

Figure 9: (a) Calculated absorbance unit by Beer-Lambert Law for *A. hydrophila* based on cell concentration. (b) Measured and calculated absorbance unit for exponential phase of *A. hydrophila*.

Table 4: Comparison between numbers of cells corresponds to the absorbance measured at 352 nm for various systems.

Phases	Number of cells based on absorbance at wavelength 352 nm (cells/mL)		
	UV spectrophotometer	Beer-Lambert	Microchannel
Lag	7.14×10^7	4.22×10^8	6.79×10^7
Exponential	1.07×10^8	6.84×10^8	1.1×10^8
Stationary	1.12×10^8	6.80×10^8	1.09×10^8

(including hydrogen bonding interactions). This can cause different charge distribution on the neighbouring species in the solution. It can result in a shift in the absorption wavelength of the analyte. Furthermore, high analyte concentrations can also alter the refractive index of the solution that could affect the absorbance obtained [43]. Deviations can also be attributed to instruments since polychromatic source of light was used in this work. The difference in the results shown in Figure 9(b) suggests different values of molar absorptivities for experimental and calculated ones that led to deviations in absorbance values obtained. Stray radiation can also be a potential source of deviations due to reflection and scattering by the surfaces of lenses, mirrors, gratings, and others.

Table 4 illustrates further the comparison between numbers of cells corresponding to the absorbance measured at 352 nm for various systems. The number of cells based on the absorbance calculated by microchannel differed slightly for all phases (~5%) when compared to the UV spectrophotometer readings. Again, the difference between the Beer-Lambert and microchannel values was larger (~84%). The above results compliment the absorbance results as discussed in Figures 7 and 8. The ability to detect low number of sample at 10^7 is quite good as well. For instances, at lag phases (Table 4), the number of cells obtained using microchannel is very close to the reading in UV spectrophotometer indirectly suggesting that this microchannel fiber optic detection is a reliable detection system for up until 10^7 cells/mL (the tested range of limit in this work). Although this detection limit is incomparable to other detection methods like PCR (DNA based) and electronic nose (volatile compounds based) that gave a detection limit of 2.5 CFU/mL [44] and 10^3 CFU/mL [45], respectively, however, this method offers advantages of being simple, easy, less laborious, and cheaper compared to the above-mentioned methods. These preliminary findings suggest further investigation should be conducted for lower detection limit in order to test and explore its capability.

The difference in absorbance between experiments and UV-Vis spectrophotometer and theoretical values might be due to the influence of external noise during experimental work. The uncertainty or disturbance in the values of absorbance may be due to the presence of impurities in the sample injected into the channel or other contaminants. Samples of biological molecules should be pure in order to quantitatively use UV absorption spectroscopy [46, 47]. Any contaminating nucleic acids in a protein sample will increase the apparent absorbance, likewise for contaminating proteins in a nucleic acid sample [48].

The optical fibers on microchannel were designed to be alignment-free. However, there were several factors that might affect the light transmission in optical system. The travelling light through fiber optical could lose power over distance. This loss of power also known as attenuation is expressed in decibels (dB) or rate of loss per unit distance. Attenuation is due to absorption by the core and cladding which might be caused by the presence of impurities and disclosing of light from the cladding. At some point, the power level may become too weak for the receiver to distinguish between the optical signal and the background noise. Consequently, it can cause signal reduction that leads to inefficiency in the system. Apart from that, macrobending of fiber optic during experiments especially to connect to the *JAZ* spectroscopy could induce the signal power loss. Further losses can also occur at the splice locations, at fiber optic connectors due to poor cleave and also presence of contaminants on the connectors [49]. As a result, all these

factors including length of fiber optic used, macrobending that occurred during connection, and link loss mechanism caused the loss of signal power to achieve higher light transmission.

Generally, in biological samples, the primary photoacceptors of UV light are nucleic acids and proteins, while visible light is absorbed by cytochromes [50]. Every sample has a different particular absorbance spectrum between UV and visible regions because it depends on the protein and DNA content of the sample [48]. Since different samples vary by their energy level, DNA, and proteins, thus special primary photoacceptors are needed for every sample to absorb most at specific spectral regions of light [51]. Besides, the characteristic and structure of each microorganism also played an important role in identification of detection region for each sample. For instance, *A. hydrophila* is a Gram-negative prokaryotic cell with straight rod with rounded ends. *A. hydrophila* contains cell wall and structure of slime-layer in matrix structure that embeds the cells. This layer or capsule also called glycocalyx is a thin layer of tangled polysaccharide fiber. The cell wall and outer membrane of *A. hydrophila* are made of thicker capsules or layers and bacteria lack of nucleus. Hence, the peak absorbance range of *A. hydrophila* falls at the UV spectral region, whereas eukaryotic microorganism contains nucleus to determine the particular spectral region of DNA peak absorption. In brief, microorganism at any phases can be detected at similar region of wavelength with difference in absorbance rate.

4. Conclusion

The detection and identification of microorganism can be done quite accurately using absorbance spectra of region. From the entire experimental work, *A. hydrophila* was detected at 350 nm to 354 nm. Besides, total volume of sample needed for detection was approximately 6 μL or 10^2 cells/mL in less than 10 minutes. These results were comparable to theoretical values and also spectrophotometer measurements. The microchannel has the potential to convey efficient, precise, and sensitive results. In a nut shell, the microchannel has proven its functionality as fiber optic biosensor which can be used for rapid and accurate detection and identification of *A. hydrophila* which would be of benefit in varieties of field. Moreover, the microchannel can be reused for other samples, is easy to move, and consists of simple methods to fabricate it. Further work needs to be done to integrate the recognition elements into a lab on chip for specific analyte of interest.

Competing Interests

The authors declare that they have no competing interests.

Acknowledgments

The authors would like to thank Malaysia Ministry of Science, Technology and Innovation for funding this project (SF-02-01-04-SF1214) and Dr. Mohd Hanif Yaacob for providing assistance needed for this research and also Dr. Zalini Yunus for providing the microbes.

References

[1] B. Austin and D. A. Austin, *Bacterial Fish Pathogens, Disease of Farmed and Wild Fish*, Springer Praxis, Godalming, UK, 4th edition, 2007.

[2] S. L. Siegel, T. L. Lewis, N. K. Tripathi, V. V. Burnley, and K. S. Latimer, "Ulcerative bacterial dermatitis of koi (*Cyprinus carpio*) and ornanmental goldfish (*Carassius auratus*)," http://www.vet.uga.edu/vpp/undergrad/sieqel/.

[3] T. D. Chugh, "Emerging and re-emerging bacterial diseases in India," *Journal of Biosciences*, vol. 33, no. 4, pp. 549–555, 2008.

[4] G. Acharya, C.-L. Chang, and C. Savran, "An optical biosensor for rapid and label-free detection of cells," *Journal of the American Chemical Society*, vol. 128, no. 12, pp. 3862–3863, 2006.

[5] J. Dupont, D. Menard, C. Herve, F. Chevalier, B. Beliaeff, and B. Minier, "Rapid estimation of *Escherichia coli* in live marine bivalve shellfish using automated conductance measurement," *Journal of Applied Microbiology*, vol. 80, pp. 81–90, 2002.

[6] Z. Yeşim Özbaş, A. Lehner, and M. Wagner, "Development of a multiplex and semi-nested PCR assay for detection of Yersinia enterocolitica and Aeromonas hydrophila in raw milk," *Food Microbiology*, vol. 17, no. 2, pp. 197–203, 2000.

[7] K. E. Rasooly, "Food microbial pathogen detection and analysis using DNA microarray technologies," *Foodborne Pathogens and Disease*, vol. 5, no. 4, pp. 531–550, 2008.

[8] S. Longyant, S. Rukpratanporn, P. Chaivisuthangkura et al., "Identification of *Vibrio* spp. in vibriosis *Penaeus vannamei* using developed monoclonal antibodies," *Journal of Invertebrate Pathology*, vol. 98, no. 1, pp. 63–68, 2008.

[9] K. Fujioka, E. Arakawa, J.-I. Kita et al., "Detection of aeromonas hydrophila in liquid media by volatile production similarity patterns, using a FF-2A electronic nose," *Sensors (Basel)*, vol. 13, no. 1, pp. 736–745, 2013.

[10] K. Thyagarajan and A. K. Ghatak, *Fiber Optic Essentials*, Wiley-Interscience, 2007.

[11] C. R. Taitt, G. P. Anderson, and F. S. Ligler, "Evanescent wave fluorescence biosensors," *Biosensors and Bioelectronics*, vol. 20, no. 12, pp. 2470–2487, 2005.

[12] J. Garaizar, A. Rementeria, and S. Porwollik, "DNA microarray technology: a new tool for the epidemiological typing of bacterial pathogens?" *FEMS Immunology and Medical Microbiology*, vol. 47, no. 2, pp. 178–189, 2006.

[13] C. E. Alupoaei and L. H. García-Rubio, "Growth behavior of microorganisms using UV-Vis spectroscopy: *Escherichia coli*," *Biotechnology and Bioengineering*, vol. 86, no. 2, pp. 163–167, 2004.

[14] C. W. Park, K. Y. Yoon, J. H. Byeon, K. Kim, and J. Hwang, "Development of rapid assessment method to determine bacterial viability based on ultraviolet and visible (UV-Vis) spectroscopy analysis including application to bioaerosols," *Aerosol and Air Quality Research*, vol. 12, no. 3, pp. 395–404, 2012.

[15] S. K. Arya, A. Singh, R. Naidoo, P. Wu, M. T. McDermott, and S. Evoy, "Chemically immobilized T4-bacteriophage for specific Escherichia coli detection using surface plasmon resonance," *Analyst*, vol. 136, no. 3, pp. 486–492, 2011.

[16] C. E. Alupoaei, J. A. Olivares, and L. H. García-Rubio, "Quantitative spectroscopy analysis of prokaryotic cells: vegetative cells and spores," *Biosensors & Bioelectronics*, vol. 19, no. 8, pp. 893–903, 2004.

[17] G. M. Whitesides, "The origins and the future of microfluidics," *Nature*, vol. 442, no. 7101, pp. 368–373, 2006.

[18] A. Manz, D. J. Harrison, E. M. J. Verpoorte et al., "Planar chips technology for miniaturization and integration of separation techniques into monitoring systems. Capillary electrophoresis on a chip," *Journal of Chromatography A*, vol. 593, no. 1-2, pp. 253–258, 1992.

[19] R. Yang and W. Wang, "Out-of-plane polymer refractive microlens fabricated based on direct lithography of SU-8," *Sensors and Actuators A: Physical*, vol. 113, no. 1, pp. 71–77, 2004.

[20] T.-K. Shih, C.-F. Chen, J.-R. Ho, and F.-T. Chuang, "Fabrication of various curved relief structures through concave surface forming and soft replica molding," *Microelectronic Engineering*, vol. 83, no. 3, pp. 471–475, 2006.

[21] H.-J. Woo, Y.-S. Kim, H.-W. Choi et al., "Optimisation of microlenses fabricated by deep proton irradiation and styrene diffusion," *Microelectronic Engineering*, vol. 57-58, pp. 945–951, 2001.

[22] V. Awatsuji, M. Sasada, N. Kawano, and T. Kubota, "Reflective microoptical element array fabricated by photofabrication technique," *Japanese Journal of Applied Physics, Part 1*, vol. 43, no. 8, pp. 5845–5849, 2004.

[23] C.-S. Lee and C.-H. Han, "A novel refractive silicon microlens array using bulk micromachining technology," *Sensors and Actuators A: Physical*, vol. 88, no. 1, pp. 87–90, 2001.

[24] Y.-Q. Fu, N. Kok, and A. Bryan, "Microfabrication of microlens array by focused ion beam technology," *Microelectronic Engineering*, vol. 54, no. 3-4, pp. 211–221, 2000.

[25] E. Gu, H. W. Choi, C. Liu et al., "Reflection/transmission confocal microscopy characterization of single-crystal diamond microlens arrays," *Applied Physics Letters*, vol. 84, no. 15, pp. 2754–2756, 2004.

[26] X. Yuan, W. X. Yu, M. He et al., "Soft-lithography-enabled fabrication of large numerical aperture refractive microlens array in hybrid SiO_2–TiO_2 sol-gel glass," *Applied Physics Letters*, vol. 86, no. 11, Article ID 114102, 2005.

[27] V. K. Parashar, A. Sayah, M. Pfeffer, F. Schoch, J. Gobrecht, and M. A. M. Gijs, "Nano-replication of diffractive optical elements in sol-gel derived glasses," *Microelectronic Engineering*, vol. 67-68, pp. 710–719, 2003.

[28] H. Wu, T. W. Odom, and G. M. Whitesides, "Reduction photolithography using microlens arrays: applications in gray scale photolithography," *Analytical Chemistry*, vol. 74, no. 14, pp. 3267–3273, 2002.

[29] A. Mazhorova, A. Markov, A. Ng et al., "Label-free bacteria detection using evanescent mode of a suspended core terahertz fiber," *Optical Society of America, Optic Express*, vol. 20, no. 5, pp. 5348–5355, 2012.

[30] A. P. Ferreira, M. M. Werneck, and R. M. Ribeiro, "Development of an evanescent-field fibre optic sensor for *Escherichia coli* O157:H7," *Biosensors and Bioelectronics*, vol. 16, no. 6, pp. 399–408, 2001.

[31] T. Geng, J. Uknalis, S.-I. Tu, and A. K. Bhunia, "Fiber-optic biosensor employing Alexa-Fluor conjugated antibody for detection of *Escherichia coli* O157:H7 from ground beef in four hours," *Sensors*, vol. 6, no. 8, pp. 796–807, 2006.

[32] A. Almadidy, J. Watterson, P. A. E. Piunno, I. V. Foulds, P. A. Horgen, and U. Krull, "A fibre-optic biosensor for detection of microbial contamination," *Canadian Journal of Chemistry*, vol. 81, no. 5, pp. 339–349, 2003.

[33] A. Leung, P. M. Shankar, and R. Mutharasan, "A review of fiber-optic biosensors," *Sensors and Actuators B: Chemical*, vol. 125, no. 2, pp. 688–703, 2007.

[34] S. Wang, X. Zhao, I. Khimji et al., "Integration of cell phone imaging with microchip ELISA to detect ovarian cancer HE4 biomarker in urine at the point-of-care," *Lab on a Chip*, vol. 11, no. 20, pp. 3411–3418, 2011.

[35] J. S. Albuquerque, M. F. Pimentel, V. L. Silva, I. M. Raimundo Jr., J. J. R. Rohwedder, and C. Pasquini, "Silicone sensing phase for detection of aromatic hydrocarbons in water employing near-infrared spectroscopy," *Analytical Chemistry*, vol. 77, no. 1, pp. 72–77, 2005.

[36] J. C. Jokerst, J. A. Adkins, B. Bisha, M. M. Mentele, L. D. Goodridge, and C. S. Henry, "Development of a paper-based analytical device for colorimetric detection of select foodborne pathogens," *Analytical Chemistry*, vol. 84, no. 6, pp. 2900–2907, 2012.

[37] P. W. Atkins and J. de Paula, *Physical Chemistry*, Oxford University Press, 2006.

[38] M. Asef Iqbal, S. G. Gupta, and S. S. Hussaini, "A review on electrochemical biosensors: principles and applications," *Advanced Biomedical Research*, vol. 3, pp. 158–163, 2012.

[39] C. E. Boyd, *Water Quality: An Introduction*, Springer, New York, NY, USA, 2015.

[40] D. N. N. Sathyanarayana and Sathyanarayana, *Electronic Absorption Spectroscopy and Related Techniques*, Universities Press, Hyderabad, India, 1st edition, 2001.

[41] C. E. Alupoaei and L. H. García-Rubio, "An interpretation model for the UV-VIS spectra of microorganisms," *Chemical Engineering Communications*, vol. 192, no. 1–3, pp. 198–218, 2005.

[42] G. P. Richards and M. A. Watson, "A simple fluorogenic method to detect *Vibrio cholerae* and *Aeromonas hydrophila* in well water for areas impacted by catastrophic disasters," *The American Journal of Tropical Medicine and Hygiene*, vol. 75, no. 3, pp. 516–521, 2006.

[43] D. A. Skoog, D. M. West, F. J. Holler, and S. R. Crouch, *Fundamentals of Analytical Chemistry*, Brooks Cole, 9th edition, 2014.

[44] M. J. Griffin, A. E. Goodwin, G. E. Merry et al., "Rapid quantitative detection of Aeromonas hydrophila strains associated with disease outbreaks in catfish aquaculture," *Journal of Veterinary Diagnostic Investigation*, vol. 25, no. 4, pp. 473–481, 2013.

[45] K. Fujioka, E. Arakawa, J.-I. Kita et al., "Detection of aeromonas hydrophila in liquid media by volatile production similarity patterns, using a FF-2A electronic nose," *Sensors*, vol. 13, no. 1, pp. 736–745, 2013.

[46] M. J. Peak, J. G. Peak, M. P. Moehring, and R. B. Webb, "Ultraviolet action spectra for DNA dimer induction, lethality, and mutagenesis in Escherichia coli with emphasis on the UVB region," *Photochemistry and Photobiology*, vol. 40, no. 5, pp. 613–620, 1984.

[47] T. Geng, M. T. Morgan, and A. K. Bhunia, "Detection of low levels of *Listeria monocytogenes* cells by using a fiber-optic immunosensor," *Applied and Environmental Microbiology*, vol. 70, no. 10, pp. 6138–6146, 2004.

[48] X. W. You, P. Huang, and S. F. Lou, "The research of fiber optic gyroscope error based on insertion loss and beam-splitting ratio of Y-waveguide," *Applied Mechanics and Materials*, vol. 182-183, pp. 606–610, 2012.

[49] O. Tiphlova and T. Karu, "Action of low-intensity laser radiation on Escherichia coli," *Critical Reviews in Biomedical Engineering*, vol. 18, no. 6, pp. 387–412, 1991.

[50] A. Belle, A. Tanay, L. Bitincka, R. Shamir, and E. K. O'Shea, "Quantification of protein half-lives in the budding yeast proteome," *Proceedings of the National Academy of Sciences of the United States of America*, vol. 103, no. 35, pp. 13004–13009, 2006.

[51] G. Wandermur, D. Rodrigues, R. Allil et al., "Plastic optical fiber-based biosensor platform for rapid cell detection," *Biosensors and Bioelectronics*, vol. 54, pp. 661–666, 2014.